Title

Microglial Inflammatory Signaling Orchestrates the Hypothalamic Immune Response to Dietary Excess and Mediates Obesity Susceptibility

Journal

Cell Metabolism, 26(1)

ISSN

1550-4131

Authors

Valdearcos, Martin
Douglass, John D
Robblee, Megan M
et al.

Publication Date

2017-07-01

DOI

10.1016/j.cmet.2017.05.015

Peer reviewed

Published in final edited form as:

Cell Metab. 2017 July 05; 26(1): 185–197.e3. doi:10.1016/j.cmet.2017.05.015.

Microglial Inflammatory Signaling Orchestrates the Hypothalamic Immune Response to Dietary Excess and Mediates Obesity Susceptibility

Martin Valdearcos[1,7], **John D. Douglass**[3,4,7], **Megan M. Robblee**[1], **Mauricio D. Dorfman**[3,4], **Daniel R. Stifler**[1], **Mariko L. Bennett**[5], **Irene Gerritse**[1,6], **Rachael Fasnacht**[3,4], **Ben A. Barres**[5], **Joshua P. Thaler**[3,4,8,*], and **Suneil K. Koliwad**[1,2,8,9,*]

[1]The Diabetes Center, University of California San Francisco, San Francisco, CA 94143, USA [2]Department of Medicine, University of California San Francisco, San Francisco, CA 94143, USA [3]University of Washington Diabetes Institute, University of Washington, Seattle, WA 98109, USA [4]Department of Medicine, University of Washington, Seattle, WA 98109, USA [5]Department of Neurobiology, Stanford University School of Medicine, Stanford, CA 94305, USA [6]Graduate School of Life Sciences, University of Utrecht, 3584 CL Utrecht, the Netherlands

SUMMARY

Dietary excess triggers accumulation of pro-inflammatory microglia in the mediobasal hypothalamus (MBH), but the components of this microgliosis and its metabolic consequences remain uncertain. Here, we show that microglial inflammatory signaling determines the immunologic response of the MBH to dietary excess and regulates hypothalamic control of energy homeostasis in mice. Either pharmacologically depleting microglia or selectively restraining microglial NF-κB-dependent signaling sharply reduced microgliosis, an effect that includes prevention of MBH entry by bone-marrow-derived myeloid cells, and greatly limited diet-induced hyperphagia and weight gain. Conversely, forcing microglial activation through cell-specific deletion of the negative NF-κB regulator A20 induced spontaneous MBH microgliosis and cellular infiltration, reduced energy expenditure, and increased both food intake and weight gain even in absence of a dietary challenge. Thus, microglial inflammatory activation, stimulated by dietary excess, orchestrates a multicellular hypothalamic response that mediates obesity susceptibility, providing a mechanistic rationale for non-neuronal approaches to treat metabolic diseases.

[*]Correspondence: jpthaler@uw.edu (J.P.T.), skoliwad@diabetes.ucsf.edu (S.K.K.).
[7]These authors contributed equally
[8]Senior author
[9]Lead Contact

AUTHOR CONTRIBUTIONS

M.V. and J.D.D. designed and conducted the experiments, analyzed data, and prepared figures. M.V. first drafted the manuscript. M.M.R., I.G., R.F., and D.R.S. assisted with key experiments. M.D.D. contributed analytically and intellectually. M.L.B. and B.A.B. provided key reagents, technical support, and expertise. S.K.K. and J.P.T. conceived of the studies, supervised their design and completion, and wrote the final manuscript. S.K.K. and M.V. prepared the final figures. J.P.T.'s laboratory conducted experiments on IKKβ^{MGKO} mice, and S.K.K.'s laboratory performed all other experiments.

SUPPLEMENTAL INFORMATION

Supplemental Information includes seven figures and one table and can be found with this article online at http://dx.doi.org/10.1016/j.cmet.2017.05.015.

In Brief

Whether hypothalamic gliosis (microglia accumulation) is a cause or a consequence of weight gain has been unclear. Valdearcos et al. show that microglia orchestrate a complex hypothalamic immune response to dietary excess. Microglial inflammatory signaling regulates both energy intake and expenditure; these cells/signaling pathways could be targeted in obesity.

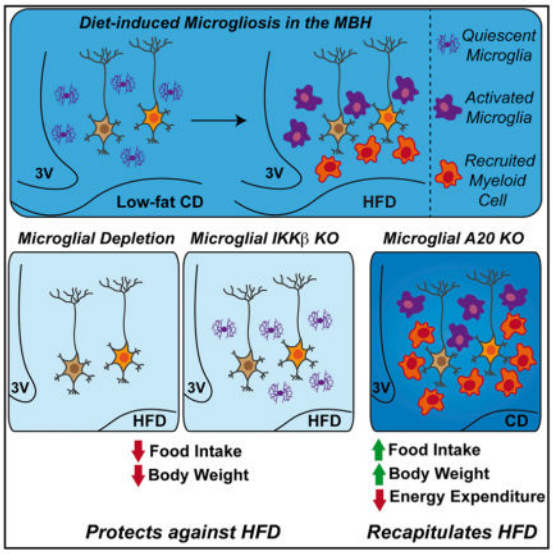

INTRODUCTION

Energy homeostasis depends on the integrated function of hypothalamic neurons that detect changes in nutrient availability through adiposity hormones, such as leptin, and coordinately control feeding behavior and metabolic rate (Schwartz et al., 2000). However, the high prevalence of obesity indicates that environmental influences, such as dietary excess, can override this control system to promote weight gain.

Clear public health concerns have spurred efforts to determine how to maintain CNS control over energy balance in the face of dietary excess. While most studies have focused on hypothalamic neurons (Waterson and Horvath, 2015), comparatively few have investigated non-neuronal cells, which outnumber neurons in the brain. Here, we provide the first mechanistic evidence that microglia, the self-renewing population of CNS macrophages, orchestrate both the immunologic and physiologic responses of the hypothalamus to dietary excess and instruct the hypo-thalamic control of food intake, energy expenditure, and body weight.

Diet-induced obesity (DIO) is associated with a form of low-grade inflammation involving macrophages and other immune cells in white adipose and other metabolic tissues and is implicated in the development of insulin resistance (Gregor and Hotamisligil, 2011). This process is paralleled by a more rapid response involving glial cell accumulation (gliosis) in the mediobasal hypothalamus (MBH), both in mice and humans (Buckman et al., 2013; Gao et al., 2014; Schur et al., 2015; Thaler et al., 2012; Valdearcos et al., 2014), and the

inflammatory activation of MBH microglia is prominent in the gliosis induced by high-fat diet (HFD) or saturated fat consumption (Thaler et al., 2012; Valdearcos et al., 2014). The porous blood-brain barrier (BBB) in the MBH may also allow infiltrating myeloid cells from the circulation to augment gliosis, as is seen in other CNS inflammatory conditions that alter BBB integrity (Ginhoux et al., 2010; Sheng et al., 2015). However, because prior analyses of "microgliosis" in mice with DIO (e.g., Thaler et al., 2012; Valdearcos et al., 2014; Morari et al., 2014) used either common myeloid markers (e.g., Iba1, CD11b, Emr1) or methods that might damage the BBB (Buckman et al., 2014), the identity of these immune cells remains uncertain.

The extent to which MBH microglial inflammatory activation regulates obesity pathogenesis also remains uncertain. On the whole, hypothalamic inflammation promotes overconsumption and weight gain in mice. For example, deleting or inhibiting the inflammatory master regulator NF-κB in neurons or astrocytes mitigated DIO while stimulating inflammation in the MBH impaired leptin and insulin signaling (Benzler et al., 2015; Douglass et al., 2017a; Zhang et al., 2008). However, these studies have not addressed the potential role of microglia in this process. Indeed microglia can initiate and orchestrate processes that either exacerbate or protect against neurotoxicity, depending on the context (Aguzzi et al., 2013). We showed that microglia mediate neuronal stress and leptin resistance due to saturated fat ingestion (Valdearcos et al., 2014) but have not yet explored their role in the more complex pathogenesis of obesity.

Here, we use multiple approaches to conditionally and specifically manipulate both the number and inflammatory activation state of resident microglia in mice. Attenuating microglial inflammatory capacity or depleting microglia altogether protects HFD-fed mice from hyperphagia and DIO and also mediates a striking reduction in microgliosis, in particular the elimination of MBH infiltration by bone-marrow-derived myeloid cells. By contrast, activating resident microglia is sufficient to trigger diet-independent weight gain and MBH recruitment of myeloid cells. Collectively, our results indicate that the inflammatory activation state of microglia controls the hypothalamic immune response to dietary excess and regulates the susceptibility to obesity.

RESULTS

Depleting CNS Resident Microglia Reduces Food Intake and Weight Gain in Mice Fed a HFD

To investigate the overall contribution of microglia to energy balance and obesity susceptibility, we fed mice either a control HFD or one containing the CSF1R inhibitor PLX5622 to selectively deplete microglia (Elmore et al., 2014). Immunostaining for the microglial marker Iba1 revealed robust depletion of microglia in the MBH of PLX5622-treated mice, whether chronically fed a standard low-fat chow diet (CD) or a HFD (Figures 1A and 1B). By contrast, PLX5622 treatment did not deplete macrophages from the white adipose tissue (WAT) of the same mice, indicating relative microglial specificity (Figure S1).

Depleting microglia significantly reduced weight gain in mice fed a HFD but not in mice fed a CD (Figure 1C). Similarly, PLX5622 treatment reduced total body fat (but not lean mass)

(Figure 1D) and food intake only in HFD-fed mice (Figures 1E and 1F). Together, these findings indicate that microglia help sustain caloric intake in the context of a HFD, thus driving increased adiposity and body weight.

Genetically Restraining the Inflammatory Responsiveness of Microglia Mitigates DIO

We sought to corroborate our findings from microglial depletion by using a genetic approach to specifically silence microglial NF-κB-mediated inflammatory signaling. Mice expressing tamoxifen-inducible Cre recombinase (CreER) in cells expressing CX3CR1 ($CX3CR1^{CreER/+}$ mice) were thus crossed with mice harboring conditional alleles of *Ikbkb*, which encodes IKKβ, an essential cofactor for NF-κB activation ($Ikbkb^{F/F}$) (Li et al., 1999). Treating the progeny with tamoxifen generated $IKK\beta^{MGKO}$ mice, in which *Ikbkb* is deleted in microglia (Figure 2A) and a subset of circulating myeloid cells (Figure S2A) (Jung et al., 2000), and $IKK\beta^{F/F}$ controls.

Cre-mediated recombination is durable in microglia, which are long lived, but transient in peripheral $CX3CR1^{+}$ cells, which are rapidly replaced by bone-marrow-derived precursors (Goldmann et al., 2013; Parkhurst et al., 2013). Thus, 4 weeks after tamoxifen treatment, *Ikbkb* mRNA levels remained reduced by ~75% in flow-sorted microglia from $IKK\beta^{MGKO}$ mice (Figures 2A and 2B) but had returned to wild-type (WT) levels in peripheral $CX3CR1^{+}$ monocytes (Figure S2A). Moreover, lipopolysaccha-ride (LPS) treatment dose dependently increased *Tnfa* (TNF) mRNA levels in microglia from $IKK\beta^{F/F}$ control mice, but not $IKK\beta^{MGKO}$ mice, indicating reduced microglial inflammatory capacity in $IKK\beta^{MGKO}$ mice (Figure 2C).

To investigate the metabolic impact of restraining microglial inflammatory activation, we studied $IKK\beta^{MGKO}$ and control mice fed either a CD or a HFD initiated 4 weeks after tamoxifen treatment. Remarkably, $IKK\beta^{MGKO}$ mice gained less weight than $IKK\beta^{F/F}$ controls specifically when fed a HFD (Figure 2D), mirroring the effect of microglial depletion (Figure 1C). Similarly, microglial IKKβ deficiency did not affect consumption of a CD (Figure 2E) but, like PLX5622 treatment, reduced cumulative intake of the HFD (Figure 2F). As before, reduced body fat accounted for the relative decrease in body weight (Figures 2G and 2H). Both $IKK\beta^{MGKO}$ and control mice had similar rates of energy expenditure (Figure 2I), suggesting that reduced food intake is primarily responsible for the lean phenotype of $IKK\beta^{MGKO}$ mice. Finally, female $IKK\beta^{MGKO}$ mice were also resistant to DIO (Figure S2).

Next, we probed the impact of microglial IKKβ deficiency on the ability of chronic dietary excess to produce microgliosis in the MBH. Compared to control mice, $IKK\beta^{MGKO}$ mice fed a HFD had consistently less microglial activation and accumulation, assessed by immunofluorescence to quantify microglial size and number (Figures 2J and 2K). Together, these analyses indicate that microglial NF-κB-dependent signaling is necessary for HFD-induced hypothalamic microgliosis, hyperphagia, and DIO.

HFD-Responsive Microgliosis Occurs in an Anatomically Specified Niche within the MBH

To investigate the cellular composition of HFD-induced MBH microgliosis, we devised a multi-parameter immunofluorescence approach to stain MBH sections. Since the common

microglial markers Iba1 and CX3CR1 are also expressed in some monocytes (CX3CR1), tissue macrophages (Iba1 and CX3CR1), and potentially perivascular CNS macrophages (CX3CR1) (Greter et al., 2015), we added two specific markers, P2Y12 and Tmem119, that are expressed exclusively by microglia (Bennett et al., 2016; Butovsky et al., 2014). Importantly, this approach also identifies the activation state of microglia, as microglial activation increases expression of Iba1 and reduces that of P2Y12 (Haynes et al., 2006) but does not alter Tmem119 or CX3CR1 levels. Therefore, using these four markers in combination assesses both the role of inflammation in HFD-induced MBH microgliosis and the cell types comprising this response.

We first confirmed that Iba1^{+} cells with an activated morphology accumulate in response to HFD consumption (4 weeks) in a cluster within the median eminence (ME) and ARC, but not the ventromedial hypothalamus (VMH; Figures 3A and 3B). By contrast, the number of MBH cells staining for either P2Y12 or Tmem119 was reduced by HFD consumption (Figures 3A and 3B). Interestingly, both P2Y12^{+} and Tmem119^{+} cells were already relatively sparse as compared to Iba1^{+} cells in the ME and ARC of CD-fed mice, but this reciprocal relationship was much more pronounced on HFD (Figures 3A and 3B).

Using CX3CR1$^{GFP/+}$ mice, we also compared the localization of cells expressing CX3CR1 in the MBH with that of cells expressing either P2Y12 or Tmem119. Mirroring the Iba1 data, this model revealed a cluster of CX3CR1-expressing (GFP^{+}) microglia induced by HFD specifically in the ME and ARC, most of which did not express P2Y12 or Tmem119 whether assessed after 4 or 8 weeks of HFD (Figures 3C and 3D). Indeed, typical double-positive resident microglia (CX3CR1^{+}/P2Y12^{+} or CX3CR1^{+}/Tmem119^{+}) were rarely seen in the cluster of microgliosis within the MBH of mice fed a HFD. Rather, their frequency increased progressively from the ME to the VMH, and they remained morphologically quiescent when compared to the cells in the ARC and ME (Figures 3C and 3D).

The MBH accumulation of Iba1- and CX3CR1-expressing cells lacking P2Y12 and Tmem119 in HFD-fed mice suggested the potential involvement of non-microglial myeloid cells in the gliosis response. Consistent with this hypothesis, HFD-fed mice had a significant rise in MBH cells expressing CD169 (Siglec1), which marks monocyte-derived cells, but not resident microglia (Butovsky et al., 2012; Gao et al., 2015) (Figures 3E and 3F). However, these CD169^{+} cells displayed a microglial morphology (Figure 3E, inset), suggesting that they may assume a hybrid, microglia-like state on arrival in the niche. Since BrdU incorporation showed no evidence for HFD-induced proliferation of resident MBH microglia (data not shown), we explored the possibility that these atypical cells might indeed be recruited from the circulation.

Peripheral Myeloid Cells Are Prominent Participants in Diet-Induced Microgliosis

We used three separate strategies to define the contribution of infiltrating cells to hypothalamic microgliosis. First, we crossed CX3CR1$^{CreER/+}$ mice with Rosa26-lox-stop-lox-tdTomato mice (Gao et al., 2015) and treated the appropriate progeny with tamoxifen to label all CX3CR1-expressing cells, including microglia. After waiting 4 weeks for peripheral immune cell replacement by unlabeled bone-marrow-derived precursors, the mice were fed a CD or HFD for an additional 4 weeks. In this model, all Iba1^{+}/tdTomato^{+} cells in

the MBH reflect resident microglia, whereas Iba1^{+}/tdTomato^{-} cells reflect myeloid cells with a more rapid turnover rate that were not present in the MBH prior to tamoxifen administration (Figure 4A). This strategy revealed a cluster of Iba1^{+}/tdTomato^{-} cells in the MBH of HFD-fed mice, supporting the concept that microgliosis includes cells recruited from a non-microglial myeloid cell pool (Figures 4B and 4C).

Second, we analyzed mice in which CX3CR1^{+} cells express GFP and CCR2^{+} cells (monocytes, but not resident microglia) express RFP (CX3CR1$^{GFP/+}$: CCR2$^{RFP/+}$) (Saederup et al., 2010). We saw that round, CCR2-expressing (RFP^{+}) cells reminiscent of monocytes appear in the MBH within a week of placing the mice on HFD (Figure S3A).

Finally, to definitively identify bone-marrow-derived cells, we lethally irradiated WT mice while shielding their heads and necks with lead to preserve BBB integrity (Mildner et al., 2007) and then performed bone marrow transplantation (BMT) with donor marrow from mice expressing ubiquitin-GFP (BMT^{GFP}) (Figure 4D). Following a 6-week recovery, we fed BMT^{GFP} and control mice a CD or HFD for 4 weeks and then scored for the presence of GFP^{+} cells in the MBH. Consistent with our prior approaches, the microgliosis induced in mice fed a HFD included a sharp increase in the number of GFP^{+} (bone-marrow-derived) cells (Figures 4E–4G and S3B).

To more specifically determine the cell types comprising HFD-induced microgliosis in BMT^{GFP} mice, we performed combined immunohistochemistry for GFP, the microglia-specific marker Tmem119, and the pan-myeloid marker CD68 (Figures 4E–4G). The GFP^{+} (bone-marrow-derived) cells in the MBH were always CD68^{+}, marking their myeloid origin, but never Tmem119^{+}, indicating that they are not typical resident microglia (Figures 4E–4G). These data together clearly indicate that HFD-induced microgliosis includes a prominent contribution from infiltrating bone-marrow-derived myeloid cells. We obtained essentially identical results when using P2Y12 to mark microglia (Figures S3C–S3E), strongly suggesting that the infiltrating cells express neither Tmem119 nor P2Y12 (Figures 4 and S3).

Our approach also revealed a population of CD68^{+} cells in the MBH that do not express Tmem119 or P2Y12 under basal CD-fed conditions, indicating that they are not typical resident microglia, and that are GFP^{-}, indicating that they are not recruited from the bone marrow (Figures 4 and S3). Some of these singly CD68^{+} cells had morphologies characteristic of local perivascular and meningeal macrophages. The number of these cells increased modestly in response to HFD, suggesting that perivascular or meningeal macrophages also contribute to diet-induced microgliosis (Figures 4 and S3). Alternatively, some of these cells may have been resident microglia that down-regulated Tmem119 and P2Y12 expression in response to HFD (Figures 4 and S3), consistent with the concomitant drop in the number of typical resident microglia (Tmem119^{+}/CD68^{+} or P2Y12^{+}/CD68^{+}) in the MBH.

Resident Microglia Control Diet-Induced Myeloid Cell Recruitment into the MBH

Given that resident microglia were required for the development of DIO in mice, we hypothesized that these cells also control peripheral myeloid cell recruitment into the MBH.

To test this, we again generated BMT^{GFP} mice and, after recovery from BMT, fed them a control or PLX5622-containing HFD. Remarkably, depleting resident microglia ($Iba1^{+}/GFP^{-}$) with PLX5622 abolished the presence of $Iba1^{+}/GFP^{+}$ cells in the MBH of mice fed a HFD, indicating that resident microglia are required to recruit these peripheral myeloid cells into the MBH (Figures 5A and 5C).

We performed two flow cytometric analyses to confirm that PLX5622 treatment did not itself impact the pool of circulating myeloid cells available to infiltrate the MBH. First, we documented that PLX5622 treatment does not affect bone-marrow-derived (GFP^{+}) cell numbers in the circulation (Figures S4A and S4B). Next, we analyzed circulating CSF1R-expressing (GFP^{+}) cells in CSF1R-eGFP ("MacGreen") mice fed a control or PLX5622-containing CD for 3 weeks (Figures S4C and S4D). Except for a slight (~30%) reduction in non-classical ($Ly6C^{Lo}$) monocytes, PLX5622 treatment had no effect on the circulating GFP^{+} pool, including neutrophils and monocyte subsets (Figures S4C and S4D). These findings corroborate recent data indicating that PLX5622 treatment in mice did not lessen brain infiltration by circulating monocytes in response to systemic TNF treatment, indicating that it does not broadly deprive these cells of their chemotactic potential (Feng et al., 2017).

We also corroborated our findings with PLX5622 by examining monocyte markers in $IKK\beta^{MGKO}$ mice. As expected, $IKK\beta^{MGKO}$ mice fed a HFD recruited fewer monocyte-derived ($CD169^{+}$) cells into the MBH than did controls (Figures 5B and 5D). These models together indicate that resident microglial activation is required for diet-induced peripheral myeloid cell recruitment into the MBH.

Genetically Potentiating NF-κB-Dependent Inflammatory Activation in Microglia Increases Diet-Induced Hypothalamic Microgliosis

We reasoned that if microglial inflammatory signaling mediates the impact of dietary excess on MBH neuronal function, then spontaneously activating microglia through genetic manipulation should be sufficient to drive both microgliosis and obesity in a diet-independent manner. To test this hypothesis, we targeted A20 (tumor necrosis factor alpha-induced protein 3 [TNFAIP3]), an anti-inflammatory molecule and primary negative regulator of NF-κB activity (Ma and Malynn, 2012). A20-deficient mice spontaneously develop neuroinflammation, which has been attributed to A20 deficiency in microglia (Guedes et al., 2014). Consistent with this, primary microglia isolated from A20-haplodeficient (*Tnfaip3*$^{+/-}$) mice had an exaggerated TNF and IL-6 secretory response to LPS and saturated fatty acid (palmitate) treatments (Figure S5A). These findings suggested that mice lacking A20 specifically in microglia might have a heightened vulnerability to HFD-induced microgliosis and metabolic dysfunction.

To delete A20 specifically in microglia, we bred $CX3CR1^{CreER/+}$ mice with those expressing a conditional allele of A20 (*Tnfaip3*$^{F/F}$) ($A20^{MGKO}$). Treating primary microglia from $A20^{MGKO}$ mice with 4-hydroxytamoxifen profoundly reduced *Tnfaip3* mRNA levels (Figure 6A), resulting in increased basal and LPS-induced TNF and IL-6 secretion *in vitro* (Figure 6B).

Based on the hypersensitivity of A20-deficient microglia to inflammatory stimuli, we analyzed MBH microgliosis in a cohort of $A20^{MGKO}$ and control mice fed a HFD beginning 4 weeks after tamoxifen administration. We first confirmed that, like $IKK\beta^{MGKO}$ mice, $A20^{MGKO}$ mice maintained microglial A20 deletion at this time point, whereas gene expression in peripheral leukocytes had returned to WT status (Figure S5B).

As predicted, $A20^{MGKO}$ mice fed a HFD had a phenotype opposite to that of $IKK\beta^{MGKO}$ mice, displaying marked increases over control mice in the number and size of microglia in the MBH, indicated by $Iba1^+$ cells bearing morphological features of inflammatory activation (Figures 6C and 6D). Moreover, the diet-induced MBH microglial accumulation in $A20^{MGKO}$ mice included substantially more infiltrating $CD169^+$ cells than in controls, a finding also opposite to the absence of these cells in $IKK\beta^{MGKO}$ mice (Figures 6E and 6F). Therefore, modulating the inflammatory activation potential of resident microglia in mice exerts reciprocal effects on microgliosis induced by HFD consumption in the MBH.

Interestingly, some $CD169^+$ cells recruited to the MBH of HFD-fed $A20^{MGKO}$ mice co-expressed Tmem119, confirming that these cells adopt features of resident microglia upon arrival in the niche (Figures 6G and 6H). Indeed, the robust MBH infiltration seen in HFD-fed $A20^{MGKO}$ mice may have induced the entering cells to undergo a more complete microglial conversion, as the analogous cells in WT mice altered their morphology and expressed both Iba1 and CX3CR1 but did not express Tmem119 (Figures 3E and 4E–4G).

Microglial A20 Deletion Induces Diet-Independent Metabolic Dysfunction

The heightened inflammatory activation state of $A20^{MGKO}$ microglia prompted us to hypothesize that $A20^{MGKO}$ mice would have an intrinsic susceptibility to obesity. In testing this hypothesis, it was critical to avoid waiting for replacement of any circulating myeloid cells that had undergone tamoxifen-induced Cre-LoxP recombination. Therefore, we performed BMT on $A20^{MGKO}$ and appropriate control mice using WT (Cre^-) donors, again employing head/neck shielding to preserve BBB integrity during irradiation (Figure 7A). After allowing time for bone marrow reconstitution, treating this model with tamoxifen deleted *Tnfaip3* exclusively in microglia ($A20^{MGKO\text{-}BMT}$). Using ubiquitin-GFP mice as BMT donors to monitor peripheral myeloid cell infiltration into the MBH, we found that tamoxifen-treated $A20^{MGKO\text{-}BMT}$ mice showed robust accumulation of GFP^+ cells in the MBH when fed only a CD (Figure S6A), indicating that microglial activation is sufficient on its own to recruit bone-marrow-derived myeloid cells into the MBH.

More impressively, the induction of microglial A20 deficiency in $A20^{MGKO\text{-}BMT}$ mice induced a spontaneous and rapid 4-fold increase in body weight gain despite being maintained on a CD (Figure 7B). This effect occurred during the first week after tamoxifen treatment and lessened over subsequent weeks. To determine the physiological mechanism for this weight gain, we analyzed energy balance in individually housed $A20^{MGKO\text{-}BMT}$ and control mice using metabolic cages. Upon tamoxifen treatment, CD-fed $A20^{MGKO\text{-}BMT}$ mice also had a 33% increase in ad libitum food intake over 4 days (Figure 7C) and concomitant reductions in VO_2 (Figure S6B), VCO_2 (Figure S6C), and energy expenditure (Figure 7E) but no differences in respiratory exchange ratio (RER) (Figure 7D) or physical activity (Figure S6D) versus control mice. Corresponding with their lower metabolic rate,

A20$^{MGKO-BMT}$ mice had reduced mRNA levels of several thermogenic genes (e.g., *Ucp1*, *Cidea*) in the brown adipose tissue (BAT), with a similar trend seen in the WAT (Figure S6E). These findings indicate that forcing microglial activation is sufficient to recapitulate key effects of HFD consumption on energy homeostasis.

The relative hyperphagia seen in A20$^{MGKO-BMT}$ mice prompted us to test their responsiveness to leptin, an important hormonal regulator of energy homeostasis. Just as chronic HFD consumption diminishes hypothalamic leptin signaling (El-Haschimi et al., 2000), deleting microglial A20 significantly reduced leptin-induced STAT3 activation in MBH neurons, even in the absence of a dietary challenge (Figures 7F and 7G). This finding suggests that the inflammatory activation of microglia increases obesity susceptibility by reducing the sensitivity of MBH neurons to homeostatic signals such as leptin.

Microglial Inflammatory Signaling Does Not Directly Affect Glucose Homeostasis or Peripheral Inflammation

Our finding that microglial inflammatory signaling regulates obesity susceptibility prompted us to test whether it may also regulate glucose homeostasis. We analyzed glucose tolerance in IKKβ^{MGKO} and A20$^{MGKO-BMT}$ mice (Figures S7A and S7B) at body weights equivalent to controls in order to avoid confounding by differential adiposity. Notably, the glucose tolerance of IKKβ^{MGKO} mice fed a HFD for 3 weeks and of A20$^{MGKO-BMT}$ mice fed a CD for 3 weeks was similar to that of corresponding diet-matched, tamoxifen-treated controls (Figures S7A and S7B).

Given that obesity induces inflammation in peripheral metabolic tissues and that the brain can modulate peripheral immunity through autonomic pathways, including some potentially involving hypothalamic neurons (Matarese et al., 2013), we tested whether microglial activation can produce peripheral inflammation. Comparing A20$^{MGKO-BMT}$ and control mice fed a CD revealed no differences in the mRNA levels of inflammatory genes in the WAT or livers (Figure S7C) or in the circulating levels of TNF and IL-6 (Figure S7D). These results both underscore cell-type specificity in the A20$^{MGKO-BMT}$ model and confirm that microglial inflammatory activation is not sufficient to directly drive peripheral tissue or systemic inflammation. Similarly, measures of peripheral tissue and systemic inflammation were not different between HFD-fed IKKβ^{MGKO} and control mice when assessed before their body weights diverged (data not shown).

DISCUSSION

Microglia rapidly accumulate in the MBH of rodents fed a HFD. However, it was previously unclear whether gliosis is a reactive consequence of weight gain or whether non-neuronal cells are instead instructive, regulating energy balance and contributing to obesity pathogenesis. Here, we provide the first definitive evidence that microglia, through their capacity for inflammatory signaling, are critical regulators of the susceptibility to DIO and an essential conduit linking dietary overconsumption to hypothalamic dysfunction.

We combine pharmacologic and genetic approaches to show that NF-κB-dependent microglial activation is critical for both the development of HFD-induced MBH

microgliosis, including the ingress of bone-marrow-derived myeloid cells, and metabolic dysfunction. Restraining this inflammatory activation in mice, either by depleting microglia or by deleting microglial *Ikbkb*, reduces food intake, mitigates DIO, and prevents MBH infiltration. By contrast, genetically activating microglia is sufficient to induce diet-independent MBH microgliosis, myeloid cell infiltration, metabolic dysfunction, and obesity. Together, these findings identify microglia as central regulators of energy balance and suggest that manipulating their activation could be an effective therapeutic for metabolic pathologies including obesity.

Prior work deleting *Ikbkb* in neurons (pan-CNS or hypothalamus only) or disrupting CNS TLR4 signaling connected hypothalamic inflammation with leptin sensitivity and DIO in mice (Kleinridders et al., 2009; Milanski et al., 2012; Zhang et al., 2008). Although these studies highlight the importance of neuronal inflammatory and/or stress signaling in DIO, the stimulus for this signaling remained unknown.

Emerging evidence suggests that non-neuronal cells may provide such a stimulus, linking diet to neuronal stress and consequent hypothalamic dysfunction (Douglass et al., 2017b; Kälin et al., 2015; Valdearcos et al., 2015). For example, we recently reported that astrocyte inflammatory signaling enhances established DIO (Douglass et al., 2017b), but its role in initiating energy imbalance was not assessed. As for microglia, we showed that they are a prerequisite for lipid-induced hypothalamic inflammation and neuronal stress (Valdearcos et al., 2014), and another recent study showed that NG2 glia maintain the dendritic processes of leptinergic neurons (Djogo et al., 2016); however, neither study reported on DIO. Here, using cell-specific mouse models, we establish that microglia not only sense pro-inflammatory signals associated with dietary excess, but also convey these signals in the MBH, modulating neuronal responsiveness to leptin and thus regulating energy homeostasis.

Whereas our findings point to a highly specialized interaction between microglia and neurons governing energy metabolism and associated behaviors, we found no weight-independent role for microglia in regulating glucose homeostasis or peripheral inflammation. These findings suggest that metabolic inflammation in peripheral tissues develops independently of the CNS, likely resulting from chronic nutrient overload and/or obesity itself. This finding may explain the slow progression of metabolic inflammation in peripheral tissues relative to the MBH and suggests the possibility of distinct sets of factors that mediate the “metabolic” activation of microglia versus peripheral macrophages.

How do activated microglia influence energy balance in the context of HFD feeding? Some insight may be gleaned from the features of $A20^{MGKO\text{-}BMT}$ mice. In particular, increased food intake in $A20^{MGKO\text{-}BMT}$ mice was associated with reduced leptin sensitivity by the MBH, and reduced whole-body energy expenditure was associated with a reduction in the mRNA levels of several thermogenic genes in the BAT, suggesting that microglial signaling may specifically interact with effector pathways of the sympathetic nervous system.

However, the specific factors mediating such microglia-neuronal cross-talk remain largely unknown. Candidate mechanisms include secreted cytokines (Guijarro et al., 2006), cell-cell interactions (Suzumura, 2013), modulation of tanycyte function (Balland et al., 2014), and

alterations to the integrity and selectivity of the BBB surrounding the MBH (Banks, 2006). Additionally, A20 is involved in cell-type-specific processes beyond controlling NF-κB activity, including autophagy, aging, and cell death (Abbasi et al., 2015). By further exploring A20 regulation of microglial function, we may uncover novel pathways and polarization states contributing to CNS metabolic regulation.

The mouse models we generated also provide important new insights into the cellular components of diet-induced microgliosis within the MBH. First, we note that the cluster of cells involved in this response is confined to the ARC and ME, whereas surrounding areas are devoid of such microgliosis. This anatomical specificity is intriguing, given that this region of the MBH is postulated to lie outside the traditional BBB (Olofsson et al., 2013), allowing cells within it to sense and respond to circulating factors, and for circulating cells to extravasate from the vasculature and join in the response.

Second, HFD-induced microgliosis in the MBH largely involves cells lacking typical definitive microglial markers such as Tmem119 and P2Y12. Indeed, based on marker analysis, the number of resident microglia in the MBH decreased in mice fed a HFD. Coincidently, however, we saw a modest rise in the number of myeloid cells in the MBH expressing neither typical microglial markers nor markers indicative of a blood-borne origin. Though their identities remain uncertain, they may represent a non-microglial, yet long-lived, population of brain-resident myeloid cells. Recently, for example, perivascular and meningeal macrophages were shown to have surprisingly slow turnover rates (Goldmann et al., 2016). Indeed, some of these “atypical” $CD68^{+}$ cells in the MBH of HFD-fed mice had morphologies suggestive of a perivascular origin, akin to cells seen at the edges of the MBH in CD-fed mice. Future work using appropriate models should attempt to define the specific contribution of perivascular and meningeal macrophages to diet-induced MBH microgliosis and hypothalamic function.

Another possibility is that these cells are actually resident microglia that downregulate typical markers in response to inflammatory activation. P2Y12 expression, for example, declines with microglial activation (Haynes et al., 2006), and many of the cells accumulating in the MBH in response to dietary excess had morphological features (shortened branches, enlarged cell bodies), suggesting cellular activation. If this were the case, then HFD-induced MBH microgliosis shifts the polarization of resident microglia but does not induce proliferation.

Whereas this conclusion is supported by our negative BrdU data, a recent study showed increased BrdU incorporation in the hypothalami of mice fed a HFD (André et al., 2017). However, whereas diet-induced microgliosis is tightly confined to the MBH, the other study described BrdU incorporation outside of this region. Also, as only Iba1 was used to mark myeloid cells, it is unclear what specific cell types were involved in that reported proliferative response. Therefore, whereas the hypothalamic response to HFD consumption may include myeloid proliferation, our data indicate that MBH-resident microglia are not involved. Rather, our findings prompt interest in determining the transcriptional signature of HFD-activated MBH microglia and whether it is different from that induced by other stimuli and from that of microglia in other brain regions.

Third, our studies clearly reveal that myeloid cells leave the circulating pool and accumulate in the MBH of HFD-fed mice. Monocyte-derived macrophages infiltrate the brain in response to a variety of inflammatory stimuli, including mouse models of traumatic brain injury and peripheral surgical trauma, and microglia may generate the chemotactic signal driving such infiltration (Feng et al., 2016; Gao et al., 2015). While prior work using bone marrow chimeras has suggested that hypothalamic infiltration by peripheral myeloid cells is also induced by HFD feeding for several months (Buckman et al., 2014; Morari et al., 2014), these studies have been inconsistent (Baufeld et al., 2016) and confounded by the effects of irradiation on BBB integrity (Diserbo et al., 2002). We overcame this potential confound in $A20^{MGKO\text{-}BMT}$ mice by using lead head/neck shielding during irradiation. However, we also observed diet-induced MBH infiltration ($CD169^{+}$ cells) in $A20^{MGKO}$ mice, which never received irradiation or BMT. Future work should focus on determining what factors induce monocyte chemotaxis into the MBH in the context of dietary excess and the metabolic impact of blocking this process.

Upon entering the MBH, infiltrating myeloid cells display morphologies characteristic of resident microglia. The fate-switching capacity of peripheral monocytes was recently described (Varvel et al., 2012), and future studies should determine its full extent in the MBH. On the other hand, this hybrid identity complicates studies to determine the independent impact of microglia versus infiltrating myeloid cells on metabolic regulation. For example, some of the GFP^{+} myeloid cells infiltrating the MBH upon deleting microglial A20 coexpress Tmem119, normally a specific marker of resident microglia. This profound phenotypic conversion could have, in turn, acted to ameliorate the amplitude and kinetics of the inflammatory and metabolic responses initiated by tamoxifen treatment in $A20^{MGKO\text{-}BMT}$ mice, especially given that the infiltrating cells expressed A20. Indeed, future work should determine whether infiltrating cells amplify MBH inflammation initiated by microglia or whether they function to quell this inflammation and hasten a return to homeostasis.

Our findings here begin to shed light on this question; it is remarkable that either treating mice with PLX5622 or deleting *Ikbkb* in microglia reduces DIO susceptibility in conjunction with abrogating peripheral cell infiltration into the MBH, whereas microglial A20 deficiency induces both metabolic dysfunction and the influx of peripheral myeloid cells into the MBH. This tight correlation between metabolic outcomes and cellular infiltration suggests that myeloid cells drawn to the MBH may indeed contribute to the pathogenesis of DIO, a hypothesis that awaits the molecular tools to independently manipulate different subtypes of myeloid cells.

In conclusion, we identify microglia as critical regulators of the hypothalamic control of energy balance and validate the concept of targeting microglia to treat obesity. In this light, it is notable that a CSF1R inhibitor highly related to PLX5622 (PLX3397) is currently being tested in human cancer trials (https://clinicaltrials.gov), potentially providing data on body weight effects in human subjects. In addition to cell depletion strategies, future therapeutics that functionally modulate microglia could offer new approaches to control energy balance and mitigate obesity and its pathologic consequences.

STAR ★ METHODS

KEY RESOURCES TABLE

REAGENT or RESOURCE	SOURCE	IDENTIFIER
Antibodies		
Rabbit polyclonal anti-Iba1	Wako	Cat# 019-19741; RRID: AB_839504
Rat monoclonal anti-CD169	Bio-Rad	Cat# MCA884; RRID: AB_322416
Rat monoclonal anti-CD68	Bio-Rad	Cat# MCA1957; RRID: AB_322219
Chicken polyclonal anti-GFP	Aves Labs	Cat# GFP-1020; RRID: AB_10000240
Rabbit polyclonal anti-RFP/TdTom	Rockland antibodies	Cat# 600-401-379; RRID: AB_2209751
Rabbit monoclonal anti-pSTAT3	Cell Signaling	Cat# 9131; RRID: AB_331586
Rabbit polyclonal anti-Caveolin-1	BD Biosciences	Cat# 610060; RRID: AB_397472
Rat monoclonal anti-F4/80	Abcam	Cat# ab6640; RRID: AB_1140040
Rabbit polyclonal anti-P2Y12	Julius lab (UCSF)	N/A
Rabbit polyclonal anti-TMEM119	Barres lab (Stanford)	N/A
PE Rat anti-mouse CD45	BD Biosciences	Cat#553081; RRID: AB_394611
FITC Rat anti-mouse CD11b	Bio-Rad	Cat# MCA74F; RRID: AB_321295
PerCP/Cy5.5 anti mouse-Ly6C	BioLegend	Cat# 128012; RRID: AB_1659241
APC anti mouse-Ly6G	eBioscience	Cat# 17-9668-80; RRID: AB_2573306
Chemicals, Peptides, Recombinant Proteins		
Tamoxifen, Free Base	MP Biomedicals	Cat# 156738
Percoll	GE Healthcare	Cat# 17-0891-02
PLX5622	Plexxikon	N/A
Critical Commercial Assays		
Mouse TNFa ELISA Ready-SET-Go Kit	eBioscience	Cat# 88-7324-88
Mouse IL-6 ELISA Ready-SET-Go Kit	eBioscience	Cat# 88-7064-88
Experimental Models: Organisms/Strains		
Mouse: B6.129P2(Cg)-*Cx3cr1*$^{tm2.1(cre/ERT2)Litt}$/WganJ	The Jackson Laboratory	JAX: 021160
Mouse: B6.129P-*Cx3cr1*^{tm1Litt}/J	The Jackson Laboratory	JAX: 005582
Mouse: C57BL/6-Tg(UBC-GFP)30Scha/J	The Jackson Laboratory	JAX: 004353
Mouse: B6.129(Cg)-*Ccr2*$^{tm2.1Ifc}$/J	The Jackson Laboratory	JAX: 017586
Mouse: B6.Cg-*Gt(ROSA)26Sor*$^{tm14(CAG-tdTomato)Hze}$/J	The Jackson Laboratory	JAX: 007914
Mouse: B6N.Cg-Tg(Csf1r-EGFP)1Hume/J	The Jackson Laboratory	JAX: 018549
Mouse: Ikbkb^{tm2Mka}	Karin Lab (UCSD)	N/A
Mouse: Tnfaip3$^{tm1.1Gvl}$	Ma Lab (UCSF)	N/A
Software and Algorithms		
FlowJo v.10	Tree Star	N/A

REAGENT or RESOURCE	SOURCE	IDENTIFIER
GraphPad Prism	GraphPad	N/A

CONTACT FOR REAGENT AND RESOURCE SHARING

Further information and requests for resources and reagents should be directed to and will be fulfilled by the Lead Contact, Suneil K. Koliwad (skoliwad@diabetes.ucsf.edu).

EXPERIMENTAL MODEL AND SUBJECT DETAILS

Mice—All studies used male C57BL/6 background mice, although we also analyzed female mice lacking microglial IKKβ in order to validate the sex-selectivity of the phenotypes in question. Mice were 8 weeks old when irradiated for bone marrow transplantation, were between 8–12 weeks old when treated with tamoxifen, and were subsequently analyzed over a period of 3 days to 12 weeks while being fed specific diets (see below). $CX3CR1^{CreER/+}$ (021160), CX3CR1-GFP (005582), UBI-GFP (004353) and Rosa26-lox-stop-lox-tdTomato (007914) mice were from The Jackson Laboratory (USA). $CX3CR1^{GFP/+}$: $CCR2^{RFP/+}$ mice were provided by Dr. Israel Charo (Saederup et al., 2010). MacGreen transgenic mice expressing eGFP under control of the *Csf1r* promoter were from the lab of Dr. Zena Werb, $Ikk\beta^{F/F}$ mice from the laboratory of Dr. Michael Karin (Arkan et al., 2005), and $Tnfaip3^{F/F}$ mice from the laboratory of Dr. Averil Ma (Tavares et al., 2010).

The appropriate progeny resulting from specific crosses of these mice, and corresponding littermate controls, received three 5 mg doses of tamoxifen (Sigma T5648) dissolved in 200 μL warm purified corn oil by enteric gavage in order to induce Cre-LoxP recombination. All mice were group housed and age-matched with ad libitum access to water and a specified diet in a pathogen-and temperature-controlled room with a 12:12h light: dark cycle. Mice were fed either a standard low-fat CD (LabDiet 5053) or a HFD (42% fat (kcal), TD. 88137; Envigo; and 60% fat (kcal), D12451, Research Diets). Microglia were depleted by administering the CSF1R inhibitor PLX5622 (Plexxikon), formulated in either a low-fat CD (AIN-76A, Research Diets) or a HFD (D12079B, Research Diets) at a dose of 1.2 g/kg. Anesthesia was by isoflurane, 100mg/kg ketamine and 10 mg/kg xylazine, or Avertin (terminal procedures).

All procedures were performed in accordance with NIH Guidelines for Care and Use of Animals and were approved by the Institutional Animal Care and Use Committees at the University of California San Francisco and the University of Washington.

METHOD DETAILS

Generation of Mouse Bone Marrow Chimeras—Bone marrow chimeras were created as described previously (Valdearcos et al., 2014). Briefly, eight-week old WT or $CX3CR1^{CreER/+}$: $A20^{F/F}$ were anesthetized and individually placed in lead tubes (RPI) to shield their heads and necks from irradiation. The mice were lethally irradiated in two 5Gy doses given 3 hr apart and underwent BMT the next day by tail-vein injection with 3×10^6 femoral and tibial bone marrow cells flushed from WT or UBI-GFP mice (to track donor-

derived myeloid cells in recipient mice). FACS was used to confirm reconstitution efficiency after a prolonged, 6 week recovery period. It is known that irradiation and BMT reduces weight gain in mice, however mice having undergone BMT still gain significantly more weight on a HFD than do untransplanted WT mice on a CD (Koliwad et al., 2010). Regardless, we included WT → WT BMT mice as controls for all experiments to account for the effect of BMT on body weight.

Measuring Food Intake and Energy Metabolism—Metabolic parameters in mice were assessed using a Comprehensive Lab Animal Monitoring System (CLAMS; Columbus Instruments) housed in the NIDDK-funded Nutrition Obesity Research Centers (NORC) metabolic core (UCSF), and the Energy Balance and Glucose Metabolism (EBGM) core (UW). Mice were singly housed and received water and food ad libitum. Cages were maintained at 20°C–22°C under a 12:12 hr light-dark cycle (light period 07:00–19:00), and mice were acclimatized for 48 hr before being studied. The cages continuously weighted food for each mouse, and daily intake was measured as change in food weight over successive 24 hr periods. Echo MRI was used to analyze body composition in conscious immobilized mice, and energy metabolic data were normalized to lean mass per the manufacturer's guideline.

Glucose Tolerance Tests—Food was removed from control, $IKK\beta^{MGKO}$ and $A20^{MGKO}$ mice 6 hr prior to assessment of glucose tolerance from 9:00AM to 3:00 PM. Mice received i.p. injections of D-glucose (2 mg/kg), followed by collection of blood by tail nick and determination of glucose levels by handheld glucometer (Abbot Diabetes Care). Total glucose area-under-curve and excursion was measured by the trapezoid rule.

Microglial Isolation—Microglial cultures were prepared as described previously (Deierborg, 2013). Briefly, cerebral cortices were harvested from mice at postnatal day 1 (P1)–P4, the meninges and blood vessels were removed, and the parenchyma minced and triturated in Dulbecco's modified Eagle's medium (DMEM) + GlutaMAX with 4.5 g/ glucose, 10% fetal bovine serum, 100U/ml penicillin, and 0.1 mg/ml streptomycin. Suspended cells were filtered (70 μm) and plated on poly-L-lysine-coated flasks. Six to 10 days later, the flasks were shaken (200 rpm) for 1hr (37°C) to specifically release microglia. Microglial cells isolated from $CX_3CR1^{CreER/+}$: $A20^{F/F}$ mice were treated with 5 μM of 4-hydroxytamoxifen for 48 hr to induce Cre-LoxP recombination. Murine hypothalamic microglia were isolated from PBS-perfused adult brains as described previously (Cardona et al., 2006). Briefly, hypothalamic tissues were digested for 30 min (37°C) with 1 mg/ml collagenase and 0.1 mg/ml DNase I, homogenized in Hank's Balanced Salt Solution, and passed through a 70-μm strainer. Cell suspensions were transferred to a Percoll discontinuous gradient (30%, 37%, 70%), and microglia-containing fractions were collected from the 70%–37% interphase after centrifugation. Microglia were immunostained with CD45-PE (553081, BD-Pharmigen) and CD11b-FITC (MCA74F; AbD-Serotec) and sorted using a FACSAria II (Becton Dickinson).

Immunohistochemistry—Anesthetized mice were perfused with saline and 4% paraformaldehyde in 100mM phosphate buffer, and their brains were dissected, postfixed in

the same fixative overnight (4°C), and immersed in 30% sucrose. Hypothalami were then separated from other regions, embedded in optimal cutting temperature compound, immediately frozen on dry ice, and stored at −80°C. Next, 35-μM-thick hypothalamic coronal sections were cut on a cryostat, blocked for 1 hr with 5% BSA in PBS containing 0.1% Triton X-100, and incubated with primary antibodies overnight at 4°C. Primary anti-mouse antibodies were against Iba1 (1:500 rabbit polyclonal; Wako), P2y12 (1:1000, kindly provided by Dr. David Julius), Tmem119 (1:500, kindly provided by Dr. Ben Barres), CD169 (1:300 rat polyclonal, Biorad), GFP (1:300 chicken polyclonal, Aves Labs), tdTomato/RFP (1:500 rabbit polyclonal, Rockland), CD68 (1:500 rat polyclonal, AbD serotec) and pSTAT3 (1:200, Cell Signaling). Epididymal white adipose tissue staining was done using the whole-mount technique as described (Martinez-Santibañez et al., 2014) with primary antibodies against caveolin-1 (1:500 rabbit polyclonal, BD BioScience) and F4/80 (1:300 rat polyclonal, Abcam). Adequate AlexaFluor-conjugated secondary antibodies were used for immunofluorescence microscopy. Sections were mounted with DAPI Vectashield solution (Vector Laboratories) to identify cell nuclei. The HRP-diaminobenzidine reaction was performed with the ABC Kit (Vector Laboratories), using biotin-labeled goat anti-rabbit IgG. Images were acquired with a confocal laser-scanning microscope (Leica TCS SP5) and Zeiss AxioImager brightfield microscope.

Cell Counting and Cell Size Determination—Iba1^{+} cells were counted manually from matched sections within prespecified regions of interest using ImageJ software. Microglial cell size was determined using a thresholding protocol (ImageJ) followed by densitometric quantification. pSTAT3-positive cells were counted from matched sections between Bregma −1.22 to −2.30 (Paxinos Mouse Brain Atlas). To determine the number of pSTAT3-positive cells in the ARC, the threshold was defined as the intensity where cells are clearly pSTAT3-positive by visual inspection.

Flow Cytometry and Cell Sorting—Blood was collected in EDTA tubes via facial vein bleed from live mice. Whole blood was stained with fluorochrome-conjugated antibodies and treated with Ammonium-Chloride-Potassium to lyse red blood cells. Cell pellets were resuspended with FACS buffer (BD bioscience), blocked (FcBlock; BD Biosciences) for 30 min, and stained (30 min) with Ly6C-PerCP/Cy5.5 (Biolegend, clone HK1.4) and Ly6G-APC (eBioscience, clone 1A8-Ly6g). CSF1R-expressing (GFP^{+}) cells in MacGreen mice were gated for viability (PI). Data were acquired on a BD LSR II flow cytometer (BD Biosciences) using “Fluorescence minus one” controls to set up gates. Data were analyzed by FlowJo v10 software (Tree Star). IKKβ^{MGKO} mice were validated by collecting tail blood from adult *Cx3cr1*$^{CreER\text{-}EYFP/+}$:*Ikbkb*$^{F/F}$ mice before and after (1 and 4 wks) TAM administration. After red blood cell lysis, eYFP^{+} monocytes were sorted by a FACSAria II (Becton Dickinson) and gated for viability (DAPI). IKKβ mRNA levels were measured in sorted cells by RT-qPCR.

Real-Time Quantitative PCR—Total RNA was extracted using Trizol or RNeasy micro kit according to manufacturers’ instructions (QIAGEN) and reverse-transcribed with High Capacity cDNA Reverse Transcription Kit (Applied Biosystems). Transcript levels were measured by semiquanti-tative real-time PCR on an ABI Prism 7900 HT (Applied

Biosystems) machine and SYBR green detection of amplicons. Data was analyzed using the sequence detection system software (SDS version 2.2; Applied Biosystems) and relative mRNA abundance was normalized to 18S. Primer sequences are listed in Table S1.

Cytokine and Chemokine Measurements—TNF and IL6 levels were measured in primary culture media by ELISA kits (eBioscience) according to the manufacturer's instructions.

QUANTIFICATION AND STATISTICAL ANALYSIS

Data are presented as mean ± SEM. Two groups were compared by unpaired two-tail Student's t test. For more than two groups, one- or two-way ANOVA was used, as appropriate, followed by Bonferroni post hoc adjustment. Repeated-measures ANOVA (RM-ANOVA) was also used whenever appropriate. All analyses used GraphPad software. $p < 0.05$ was considered significant.

Supplementary Material

Refer to Web version on PubMed Central for supplementary material.

Acknowledgments

We thank Plexxikon and Dr. Brian West for PLX5622. This work was supported by the American Diabetes Association (Pathway Award 1-14-ACE-51 to J.P.T.), the NIDDK (K08 DK088872 to J.P.T., T32 DK7247-37 and F32 DK108473-01 to J.D.D., and R01 DK103175-02 to S.K.K.), and a UCSF Diabetes Family Fund Award to M.V. Metabolic phenotyping was assisted by the Nutrition Obesity Research Centers at UCSF (DK098722) and The University of Washington (DK035816), and the Diabetes Research Center at The University of Washington (DK017047).

References

Abbasi A, Forsberg K, Bischof F. The role of the ubiquitin-editing enzyme A20 in diseases of the central nervous system and other pathological processes. Front Mol Neurosci. 2015; 8:21. [PubMed: 26124703]

Aguzzi A, Barres BA, Bennett ML. Microglia: scapegoat, saboteur, or something else? Science. 2013; 339:156–161. [PubMed: 23307732]

André C, Guzman-Quevedo O, Rey C, Rémus-Borel J, Clark S, Castellanos-Jankiewicz A, Ladeveze E, Leste-Lasserre T, Nadjar A, Abrous DN, et al. Inhibiting microglia expansion prevents diet-induced hypothalamic and peripheral inflammation. Diabetes. 2017; 66:908–919. [PubMed: 27903745]

Arkan MC, Hevener AL, Greten FR, Maeda S, Li ZW, Long JM, Wynshaw-Boris A, Poli G, Olefsky J, Karin M. IKK-beta links inflammation to obesity-induced insulin resistance. Nat Med. 2005; 11:191–198. [PubMed: 15685170]

Balland E, Dam J, Langlet F, Caron E, Steculorum S, Messina A, Rasika S, Falluel-Morel A, Anouar Y, Dehouck B, et al. Hypothalamic tanycytes are an ERK-gated conduit for leptin into the brain. Cell Metab. 2014; 19:293–301. [PubMed: 24506870]

Banks WA. Blood-brain barrier and energy balance. Obesity (Silver Spring). 2006; 14(Suppl 5):234S–237S. [PubMed: 17021373]

Baufeld C, Osterloh A, Prokop S, Miller KR, Heppner FL. High-fat diet-induced brain region-specific phenotypic spectrum of CNS resident microglia. Acta Neuropathol. 2016; 132:361–375. [PubMed: 27393312]

Bennett ML, Bennett FC, Liddelow SA, Ajami B, Zamanian JL, Fernhoff NB, Mulinyawe SB, Bohlen CJ, Adil A, Tucker A, et al. New tools for studying microglia in the mouse and human CNS. Proc Natl Acad Sci USA. 2016; 113:E1738–E1746. [PubMed: 26884166]

Benzler J, Ganjam GK, Pretz D, Oelkrug R, Koch CE, Legler K, Stöhr S, Culmsee C, Williams LM, Tups A. Central inhibition of IKKβ/NF-κB signaling attenuates high-fat diet-induced obesity and glucose intolerance. Diabetes. 2015; 64:2015–2027. [PubMed: 25626735]

Buckman LB, Thompson MM, Moreno HN, Ellacott KL. Regional astrogliosis in the mouse hypothalamus in response to obesity. J Comp Neurol. 2013; 521:1322–1333. [PubMed: 23047490]

Buckman LB, Hasty AH, Flaherty DK, Buckman CT, Thompson MM, Matlock BK, Weller K, Ellacott KL. Obesity induced by a high-fat diet is associated with increased immune cell entry into the central nervous system. Brain Behav Immun. 2014; 35:33–42. [PubMed: 23831150]

Butovsky O, Siddiqui S, Gabriely G, Lanser AJ, Dake B, Murugaiyan G, Doykan CE, Wu PM, Gali RR, Iyer LK, et al. Modulating inflammatory monocytes with a unique microRNA gene signature ameliorates murine ALS. J Clin Invest. 2012; 122:3063–3087. [PubMed: 22863620]

Butovsky O, Jedrychowski MP, Moore CS, Cialic R, Lanser AJ, Gabriely G, Koeglsperger T, Dake B, Wu PM, Doykan CE, et al. Identification of a unique TGF-β-dependent molecular and functional signature in microglia. Nat Neurosci. 2014; 17:131–143. [PubMed: 24316888]

Cardona AE, Huang D, Sasse ME, Ransohoff RM. Isolation of murine microglial cells for RNA analysis or flow cytometry. Nat Protoc. 2006; 1:1947–1951. [PubMed: 17487181]

Deierborg T. Preparation of primary microglia cultures from postnatal mouse and rat brains. Methods Mol Biol. 2013; 1041:25–31. [PubMed: 23813366]

Diserbo M, Agin A, Lamproglou I, Mauris J, Staali F, Multon E, Amourette C. Blood-brain barrier permeability after gamma whole-body irradiation: an in vivo microdialysis study. Can J Physiol Pharmacol. 2002; 80:670–678. [PubMed: 12182325]

Djogo T, Robins SC, Schneider S, Kryzskaya D, Liu X, Mingay A, Gillon CJ, Kim JH, Storch KF, Boehm U, et al. Adult NG2-glia are required for median eminence-mediated leptin sensing and body weight control. Cell Metab. 2016; 23:797–810. [PubMed: 27166944]

Douglass JD, Dorfman MD, Fasnacht R, Shaffer LD, Thaler JP. Astrocyte IKKβ/NF-κB signaling is required for diet-induced obesity and hypothalamic inflammation. Mol Metab. 2017a; 6:366–373. [PubMed: 28377875]

Douglass JD, Dorfman MD, Thaler JP. Glia: silent partners in energy homeostasis and obesity pathogenesis. Diabetologia. 2017b; 60:226–236. [PubMed: 27986987]

El-Haschimi K, Pierroz DD, Hileman SM, Bjørbaek C, Flier JS. Two defects contribute to hypothalamic leptin resistance in mice with diet-induced obesity. J Clin Invest. 2000; 105:1827–1832. [PubMed: 10862798]

Elmore MR, Najafi AR, Koike MA, Dagher NN, Spangenberg EE, Rice RA, Kitazawa M, Matusow B, Nguyen H, West BL, Green KN. Colony-stimulating factor 1 receptor signaling is necessary for microglia viability, unmasking a microglia progenitor cell in the adult brain. Neuron. 2014; 82:380–397. [PubMed: 24742461]

Feng X, Jopson TD, Paladini MS, Liu S, West BL, Gupta N, Rosi S. Colony-stimulating factor 1 receptor blockade prevents fractionated whole-brain irradiation-induced memory deficits. J Neuroinflammation. 2016; 13:215. [PubMed: 27576527]

Feng X, Valdearcos M, Uchida Y, Lutrin D, Maze M, Koliwad SK. Microglia mediate postoperative hippocampal inflammation and cognitive decline in mice. JCI Insight. 2017; 2:e91229. [PubMed: 28405620]

Gao Y, Ottaway N, Schriever SC, Legutko B, García-Cáceres C, de la Fuente E, Mergen C, Bour S, Thaler JP, Seeley RJ, et al. Hormones and diet, but not body weight, control hypothalamic microglial activity. Glia. 2014; 62:17–25. [PubMed: 24166765]

Gao L, Brenner D, Llorens-Bobadilla E, Saiz-Castro G, Frank T, Wieghofer P, Hill O, Thiemann M, Karray S, Prinz M, et al. Infiltration of circulating myeloid cells through CD95L contributes to neurode-generation in mice. J Exp Med. 2015; 212:469–480. [PubMed: 25779632]

Ginhoux F, Greter M, Leboeuf M, Nandi S, See P, Gokhan S, Mehler MF, Conway SJ, Ng LG, Stanley ER, et al. Fate mapping analysis reveals that adult microglia derive from primitive macrophages. Science. 2010; 330:841–845. [PubMed: 20966214]

Goldmann T, Wieghofer P, Müller PF, Wolf Y, Varol D, Yona S, Brendecke SM, Kierdorf K, Staszewski O, Datta M, et al. A new type of microglia gene targeting shows TAK1 to be pivotal in CNS autoimmune inflammation. Nat Neurosci. 2013; 16:1618–1626. [PubMed: 24077561]

Goldmann T, Wieghofer P, Jordão MJ, Prutek F, Hagemeyer N, Frenzel K, Amann L, Staszewski O, Kierdorf K, Krueger M, et al. Origin, fate and dynamics of macrophages at central nervous system interfaces. Nat Immunol. 2016; 17:797–805. [PubMed: 27135602]

Gregor MF, Hotamisligil GS. Inflammatory mechanisms in obesity. Annu Rev Immunol. 2011; 29:415–445. [PubMed: 21219177]

Greter M, Lelios I, Croxford AL. Microglia versus myeloid cell nomenclature during brain inflammation. Front Immunol. 2015; 6:249. [PubMed: 26074918]

Guedes RP, Csizmadia E, Moll HP, Ma A, Ferran C, da Silva CG. A20 deficiency causes spontaneous neuroinflammation in mice. J Neuroinflammation. 2014; 11:122. [PubMed: 25026958]

Guijarro A, Laviano A, Meguid MM. Hypothalamic integration of immune function and metabolism. Prog Brain Res. 2006; 153:367–405. [PubMed: 16876587]

Haynes SE, Hollopeter G, Yang G, Kurpius D, Dailey ME, Gan WB, Julius D. The P2Y12 receptor regulates microglial activation by extracellular nucleotides. Nat Neurosci. 2006; 9:1512–1519. [PubMed: 17115040]

Jung S, Aliberti J, Graemmel P, Sunshine MJ, Kreutzberg GW, Sher A, Littman DR. Analysis of fractalkine receptor CX(3)CR1 function by targeted deletion and green fluorescent protein reporter gene insertion. Mol Cell Biol. 2000; 20:4106–4114. [PubMed: 10805752]

Kälin S, Heppner FL, Bechmann I, Prinz M, Tschöp MH, Yi CX. Hypothalamic innate immune reaction in obesity. Nat Rev Endocrinol. 2015; 11:339–351. [PubMed: 25824676]

Kleinridders A, Schenten D, Könner AC, Belgardt BF, Mauer J, Okamura T, Wunderlich FT, Medzhitov R, Brüning JC. MyD88 signaling in the CNS is required for development of fatty acid-induced leptin resistance and diet-induced obesity. Cell Metab. 2009; 10:249–259. [PubMed: 19808018]

Koliwad SK, Streeper RS, Monetti M, Cornelissen I, Chan L, Terayama K, Naylor S, Rao M, Hubbard B, Farese RV Jr. DGAT1-dependent triacylglycerol storage by macrophages protects mice from diet-induced insulin resistance and inflammation. J Clin Invest. 2010; 120:756–767. [PubMed: 20124729]

Li ZW, Chu W, Hu Y, Delhase M, Deerinck T, Ellisman M, Johnson R, Karin M. The IKKbeta subunit of IkappaB kinase (IKK) is essential for nuclear factor kappaB activation and prevention of apoptosis. J Exp Med. 1999; 189:1839–1845. [PubMed: 10359587]

Ma A, Malynn BA. A20: linking a complex regulator of ubiquitylation to immunity and human disease. Nat Rev Immunol. 2012; 12:774–785. [PubMed: 23059429]

Martinez-Santibañez G, Cho KW, Lumeng CN. Imaging white adipose tissue with confocal microscopy. Methods Enzymol. 2014; 537:17–30. [PubMed: 24480339]

Matarese G, Procaccini C, Menale C, Kim JG, Kim JD, Diano S, Diano N, De Rosa V, Dietrich MO, Horvath TL. Hunger-promoting hypothalamic neurons modulate effector and regulatory T-cell responses. Proc Natl Acad Sci USA. 2013; 110:6193–6198. [PubMed: 23530205]

Milanski M, Arruda AP, Coope A, Ignacio-Souza LM, Nunez CE, Roman EA, Romanatto T, Pascoal LB, Caricilli AM, Torsoni MA, et al. Inhibition of hypothalamic inflammation reverses diet-induced insulin resistance in the liver. Diabetes. 2012; 61:1455–1462. [PubMed: 22522614]

Mildner A, Schmidt H, Nitsche M, Merkler D, Hanisch UK, Mack M, Heikenwalder M, Brück W, Priller J, Prinz M. Microglia in the adult brain arise from Ly-6ChiCCR2+ monocytes only under defined host conditions. Nat Neurosci. 2007; 10:1544–1553. [PubMed: 18026096]

Morari J, Anhe GF, Nascimento LF, de Moura RF, Razolli D, Solon C, Guadagnini D, Souza G, Mattos AH, Tobar N, et al. Fractalkine (CX3CL1) is involved in the early activation of hypothalamic inflammation in experimental obesity. Diabetes. 2014; 63:3770–3784. [PubMed: 24947351]

Olofsson LE, Unger EK, Cheung CC, Xu AW. Modulation of AgRP-neuronal function by SOCS3 as an initiating event in diet-induced hypothalamic leptin resistance. Proc Natl Acad Sci USA. 2013; 110:E697–E706. [PubMed: 23386726]

Parkhurst CN, Yang G, Ninan I, Savas JN, Yates JR 3rd, Lafaille JJ, Hempstead BL, Littman DR, Gan WB. Microglia promote learning-dependent synapse formation through brain-derived neurotrophic factor. Cell. 2013; 155:1596–1609. [PubMed: 24360280]

Saederup N, Cardona AE, Croft K, Mizutani M, Cotleur AC, Tsou CL, Ransohoff RM, Charo IF. Selective chemokine receptor usage by central nervous system myeloid cells in CCR2-red fluorescent protein knock-in mice. PLoS One. 2010; 5:e13693. [PubMed: 21060874]

Schur EA, Melhorn SJ, Oh SK, Lacy JM, Berkseth KE, Guyenet SJ, Sonnen JA, Tyagi V, Rosalynn M, De Leon B, et al. Radiologic evidence that hypothalamic gliosis is associated with obesity and insulin resistance in humans. Obesity (Silver Spring). 2015; 23:2142–2148. [PubMed: 26530930]

Schwartz MW, Woods SC, Porte D Jr, Seeley RJ, Baskin DG. Central nervous system control of food intake. Nature. 2000; 404:661–671. [PubMed: 10766253]

Sheng J, Ruedl C, Karjalainen K. Most tissue-resident macrophages except microglia are derived from fetal hematopoietic stem cells. Immunity. 2015; 43:382–393. [PubMed: 26287683]

Suzumura A. Neuron-microglia interaction in neuroinflammation. Curr Protein Pept Sci. 2013; 14:16–20. [PubMed: 23544747]

Tavares RM, Turer EE, Liu CL, Advincula R, Scapini P, Rhee L, Barrera J, Lowell CA, Utz PJ, Malynn BA, Ma A. The ubiquitin modifying enzyme A20 restricts B cell survival and prevents autoimmunity. Immunity. 2010; 33:181–191. [PubMed: 20705491]

Thaler JP, Yi CX, Schur EA, Guyenet SJ, Hwang BH, Dietrich MO, Zhao X, Sarruf DA, Izgur V, Maravilla KR, et al. Obesity is associated with hypothalamic injury in rodents and humans. J Clin Invest. 2012; 122:153–162. [PubMed: 22201683]

Valdearcos M, Robblee MM, Benjamin DI, Nomura DK, Xu AW, Koliwad SK. Microglia dictate the impact of saturated fat consumption on hypothalamic inflammation and neuronal function. Cell Rep. 2014; 9:2124–2138. [PubMed: 25497089]

Valdearcos M, Xu AW, Koliwad SK. Hypothalamic inflammation in the control of metabolic function. Annu Rev Physiol. 2015; 77:131–160. [PubMed: 25668019]

Varvel NH, Grathwohl SA, Baumann F, Liebig C, Bosch A, Brawek B, Thal DR, Charo IF, Heppner FL, Aguzzi A, et al. Microglial repopulation model reveals a robust homeostatic process for replacing CNS myeloid cells. Proc Natl Acad Sci USA. 2012; 109:18150–18155. [PubMed: 23071306]

Waterson MJ, Horvath TL. Neuronal regulation of energy homeostasis: beyond the hypothalamus and feeding. Cell Metab. 2015; 22:962–970. [PubMed: 26603190]

Zhang X, Zhang G, Zhang H, Karin M, Bai H, Cai D. Hypothalamic IKKbeta/NF-kappaB and ER stress link overnutrition to energy imbalance and obesity. Cell. 2008; 135:61–73. [PubMed: 18854155]

Highlights

- Microglia orchestrate a multicellular hypothalamic immune response to dietary excess
- Restraining microglial activation in mice prevents this response and lessens obesity
- Forcing the activation of microglia disrupts energy balance to induce weight gain
- Microglia thus offer a non-neuronal CNS target to curb obesity and its consequences

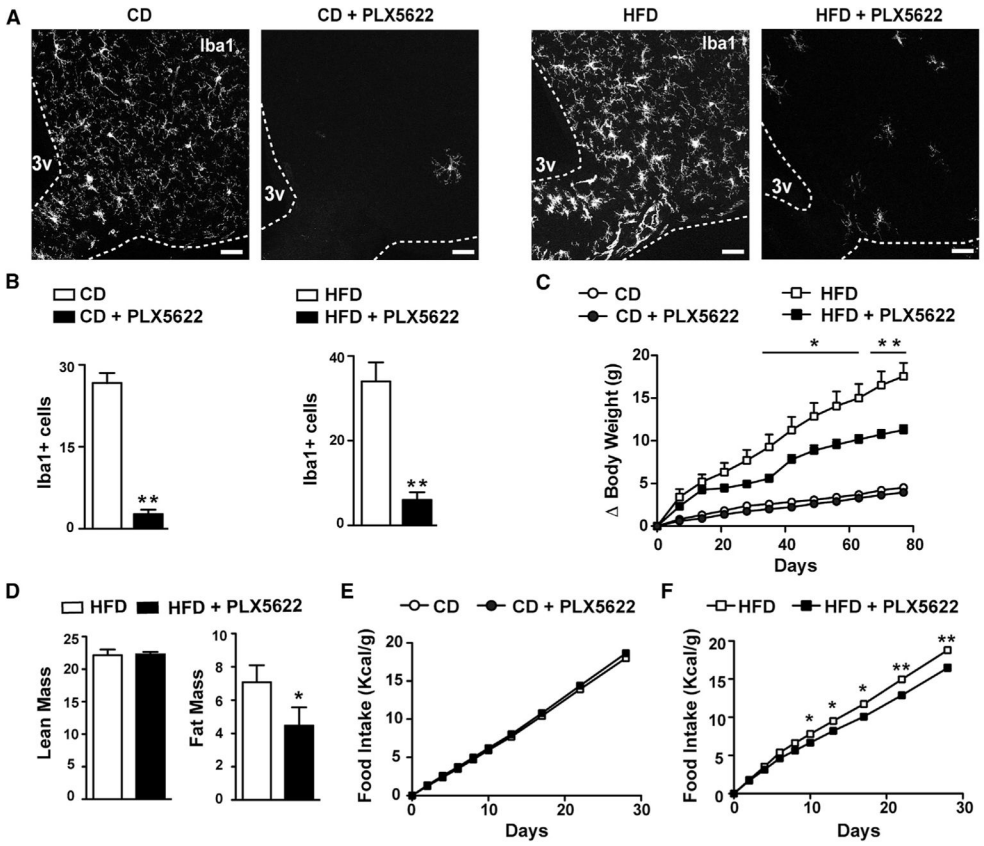

Figure 1. Microglial Depletion Reduces Body Weight and Food Intake in Mice Fed a HFD

(A) Representative MBH sections showing Iba1^{+} microglial depletion by feeding mice either a CD or a HFD containing PLX5622 (1.2 g/kg) versus a nutrient-matched control diet.

(B) Quantification of (A) (n = 6–8, two-tailed t test, **p < 0.01 versus control).

(C) Reduced body weight in PLX5622-treated mice, specifically when fed a HFD (n = 12, two-way repeated-measures [RM] ANOVA, *p < 0.05 or **p < 0.01 HFD versus HFD+ PLX5622).

(D) Unchanged lean mass and reduced fat mass in PLX5622-treated mice fed a 4-week HFD (n = 12, two-tailed t test, *p < 0.05 versus HFD).

(E) Equivalent food intake in PLX5622-treated and control mice fed a low-fat CD.

(F) Reduced food intake in PLX5622-treated mice fed a HFD (cumulative intake normalized to intial body weight, n = 12, two-way RM-ANOVA, *p < 0.05 or **p < 0.01 versus HFD).

Values are mean ± SEM (3V, third ventricle; scale bar, 20 μm). See also Figure S1.

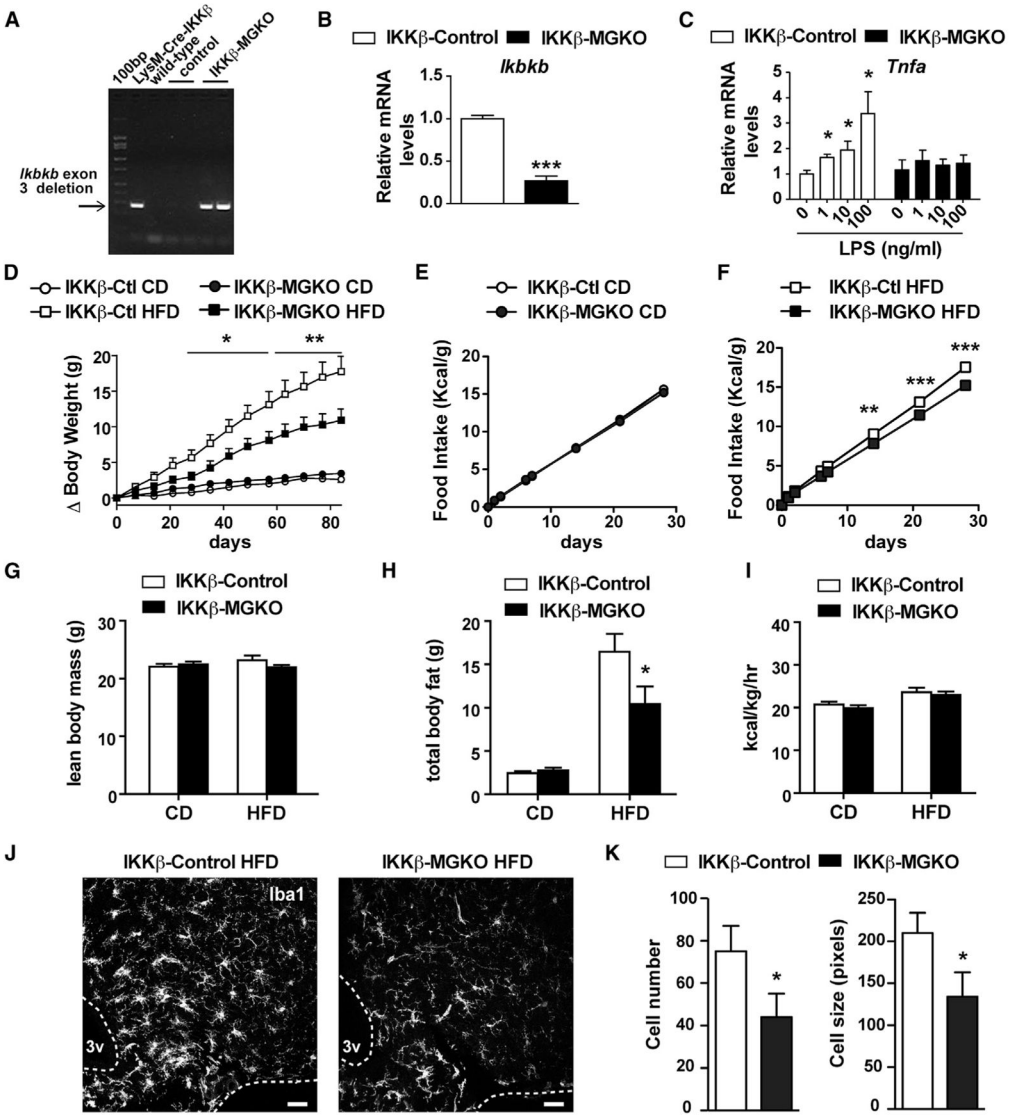

Figure 2. Deleting Microglial IKKβ Reduces Body Weight and Food Intake in Mice Fed a HFD

(A and B) Genomic PCR for truncated IKKβ exon 3 (A) and qPCR for *Ikbkb* mRNA (B) from sorted CD11b^{+}/CD45^{low} microglia 4 weeks after tamoxifen-induced recombination (n = 5–7, two-tailed t test; ***p < 0.001).

(C) *Tnfa* (TNF) mRNA induction in extracted microglia treated with LPS *ex vivo* showing reduced response in IKKβ^{MGKO} microglia (n = 4, two-tailed t test; *p < 0.05 versus non-LPS control).

(D) Reduced body weight in IKKβ^{MGKO} mice fed a HFD (n = 12–16; two-way RM-ANOVA, *p < 0.05, **p < 0.01 KO HFD versus Ctl HFD).

(E) Equivalent food intake in IKKβ^{MGKO} and control mice fed a CD (n = 5–6).

(F) Reduced food intake in IKKβ^{MGKO} mice fed a HFD (cumulative intake normalized to intial body weight, n = 6–7; two-way RM-ANOVA; **p < 0.01, ***p < 0.001).

(G) Equivalent lean body mass in IKKβ^{MGKO} and control mice fed a CD and HFD (n = 10–12).

(H) Reduced total body fat in IKKβ^{MGKO} mice fed a HFD (n = 10–12/group; two-way ANOVA; *p < 0.05 KO HFD versus Ctl HFD).
(I) Equivalent energy expenditure in IKKβ^{MGKO} and control mice (n = 8).
(J) Reduced number and size of Iba1^{+} microglia in the hypothalami of IKKβ^{MGKO} mice fed a HFD. Values are mean ± SEM (scale bar, 20 μm).
(K) Quantification of (J). Values are mean ± SEM. *p < 0.05 versus control. See also Figures S2 and S7.

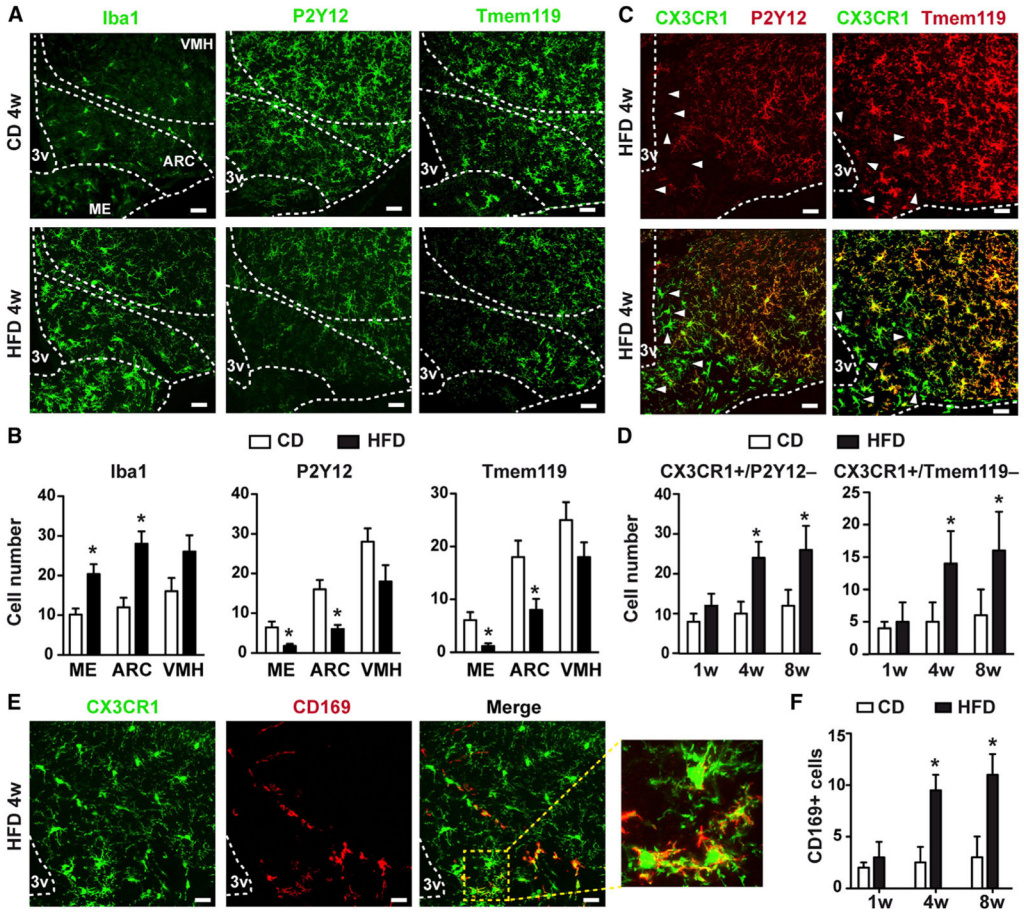

Figure 3. Diet-Responsive Microglia Are Spatially Distinct within the Hypothalamus

(A) MBH sections showing a distinct spatial distribution of Iba1^{+}, P2Y12^{+}, and Tmem119^{+} cells in the median eminence (ME), arcuate nucleus (ARC), and ventromedial hypothalamus (VMH).

(B) Quantification of (A).

(C) Representative hypothalamic sections stained for P2Y12 or Tmem119 showing lack of co-localization with GFP (arrowheads) in CX3CR1-GFP mice following a 4-week HFD.

(D) Increased hypothalamic CX3CR1^{+}/P2Y12^{-} and Cx3cr1^{+}/Tmem119^{-} cell numbers in response to HFD.

(E) Representative sections showing that a 4-week HFD induces MBH infiltration by CD169^{+} monocytes acquiring a microglia-like morphology on arrival in the niche (inset).

(F) Quantification of HFD-induced CD169^{+} MBH infiltration. Values are mean ± SEM (n = 8, *$p < 0.05$ versus CD; 3V, third ventricle; scale bar, 20 μm).

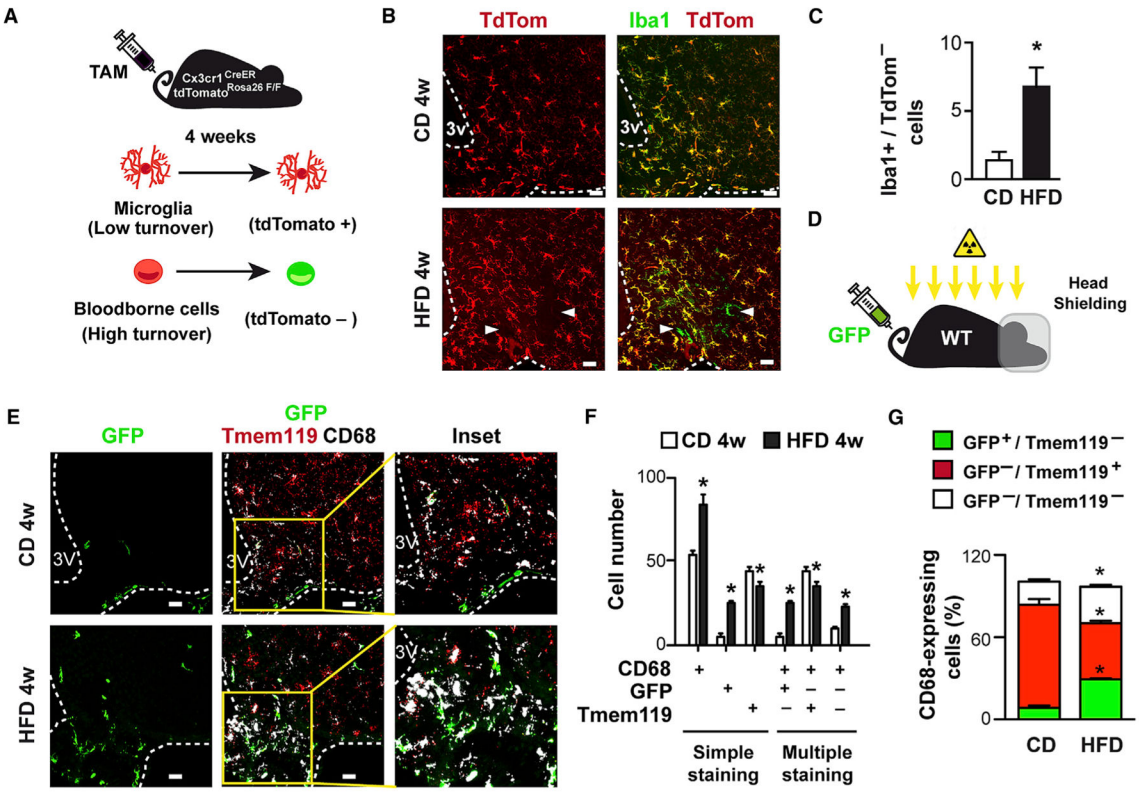

Figure 4. Peripheral Myeloid Cells Recruited to the MBH Participate in Diet-Induced Microgliosis

(A) Scheme to distinguish between resident microglia and infiltrating cells using CX3CR1$^{CreER/+}$: Rosa26-lox-stop-lox-tdTomato mice. 4 weeks after tamoxifen-induced Cre-LoxP recombination, microglia are tdTomato^{+} while circulating monocytes are tdTomato^{-}.

(B) Representative Iba1^{+}/tdTomato^{-} cells, indicating their blood-borne origin (arrowheads), at the edges of the MBH in mice generated as in (A).

(C) Increased MBH parenchymal infiltration by Iba1^{+}/tdTomato^{-} cells in response to HFD.

(D) Bone marrow transplantation strategy to reconstitute irradiated mice (with head shielding) with ubiquitin-GFP marrow (BMT^{GFP}).

(E) Representative hypothalamic sections from BMT^{GFP} mice fed a CD or HFD for 4 weeks and stained for markers of bone-marrow-derived infiltrating cells (GFP), resident microglia (Tmem119), and pan-myeloid identity (CD68), showing marked diet-induced myeloid cell infiltration (GFP^{+}/CD68^{+}/Tmem119^{-}) and an increased number of atypical myeloid cells (CD68^{+}/GFP^{-}/Tmem119^{-}) in the MBH (see insets).

(F) Data from singly and multiply stained MBH sections in (E), quantifying increased absolute numbers of total CD68^{+} cells, infiltrating myeloid cells and atypical myeloid cells, and a decreased number of resident microglia (Tmem119^{+}) in response to a HFD ([+], positive staining by indicated antibody; [−], negative staining by indicated antibody; [blank], unstained for indicated antibody).

(G) Quantification of the relative myeloid (CD68^{+}) composition of the MBH from sections in (E), showing a diet-induced emergence of infiltrating cells (GFP^{+}/Tmem119^{-}) cells, a

decrease in the contribution of resident yolk sac-derive microglia ($GFP^{-}/Tmem119^{+}$), and an increase in the contribution of atypical microglia/hypothalamic macrophages ($CD68^{+}$ cells negative for the other two markers). Values are mean ± SEM (n = 6–8, *p < 0.05 versus CD; 3V, third ventricle; scale bar, 20 μm). See also Figure S3.

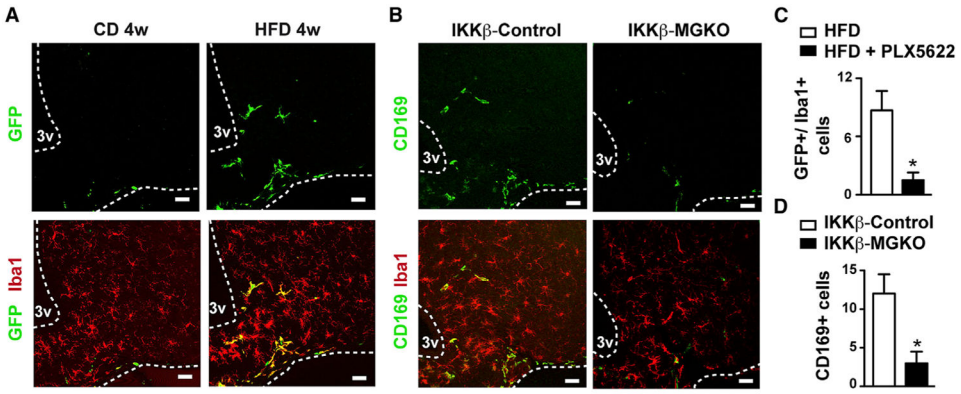

Figure 5. Depleting Microglia or Restraining Their Activation Potential Abolishes HFD-Induced Myeloid Cell Infiltration into the MBH

(A) Representative sections showing that PLX5622-induced depletion of microglia ($Iba1^{+}$) abolishes bone-marrow-derived (GFP^{+}) cell recruitment into the MBH of HFD-fed mice.

(B) Similar impact on HFD-induced $CD169^{+}$ cell infiltration into the MBH of $IKK\beta^{MGKO}$ mice.

(C) Quantification of (A).

(D) Quantification of (B). Values are mean ± SEM (n = 6–8, *p < 0.05; 3V, third ventricle; scale bar, 20 μm). See also Figure S4.

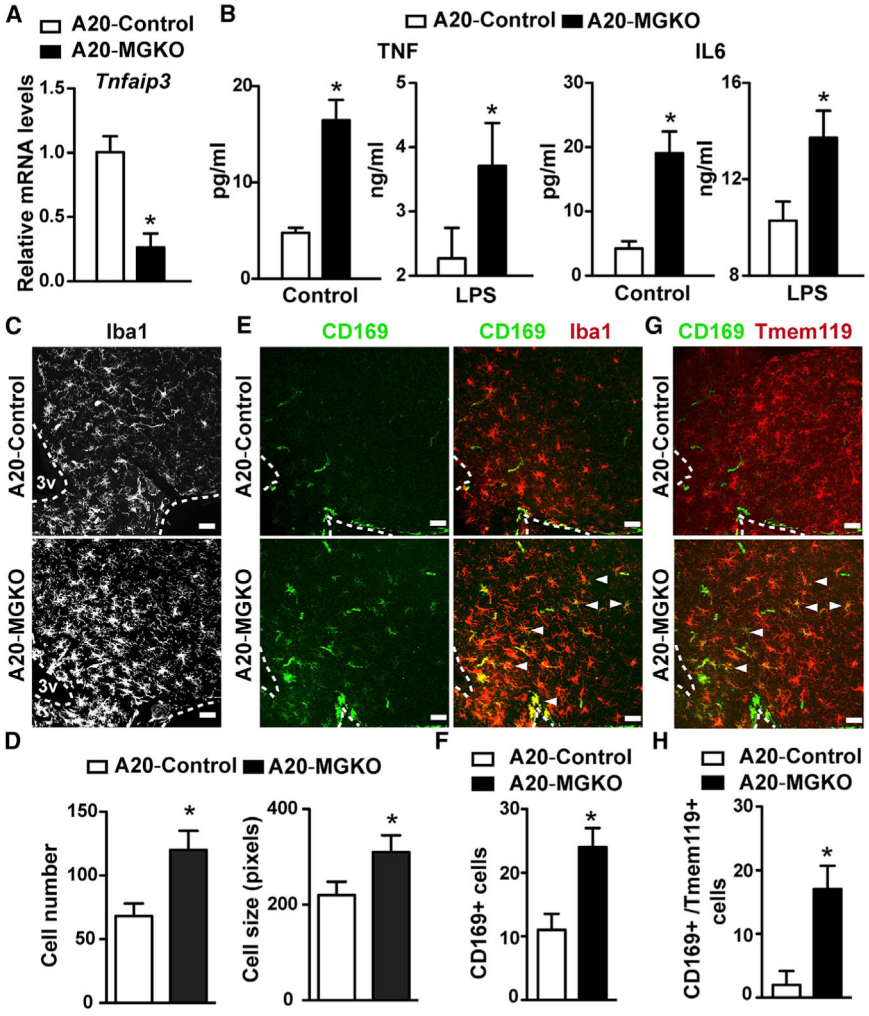

Figure 6. Deleting Microglial *Tnfaip3* Increases Inflammatory Activation and Hypo-thalamic Microgliosis in Response to HFD

(A) Reduced *Tnfaip3* (A20) mRNA levels in the $A20^{MGKO}$ microglia. *$p < 0.05$ versus control.

(B) Increased TNF and IL-6 secretion by microglia isolated from $Cx3cr1^{CreER/+}$: $A20^{F/F}$ ($A20^{MGKO}$) mice, treated with 4-hydroxytamoxifen (5 μM, 48 hr), and then treated with LPS (100 ng/mL, 16 hr) (n = 5, *$p < 0.05$ versus control).

(C) Increased number and size of $Iba1^{+}$ microglia in the MBH of $A20^{MGKO}$ mice fed a HFD for 4 weeks.

(D) Quantification of (C) (n = 6, *$p < 0.05$ versus control).

(E) Increased infiltration of $CD169^{+}$ cells showing co-localization with the marker Iba1 (arrowheads) into the MBH of $A20^{MGKO}$ fed a HFD for 4 weeks.

(F) Quantification of (E).

(G) Co-localization of CD169 with the microglial marker Tmem119 (arrowheads) in the MBH of $A20^{MGKO}$ mice fed a HFD for 4 weeks.

(H) Quantification of (G). Values are mean ± SEM (n = 6–8, *$p < 0.05$ versus control; 3V, third ventricle; scale bar, 20 μm). See also Figure S5.

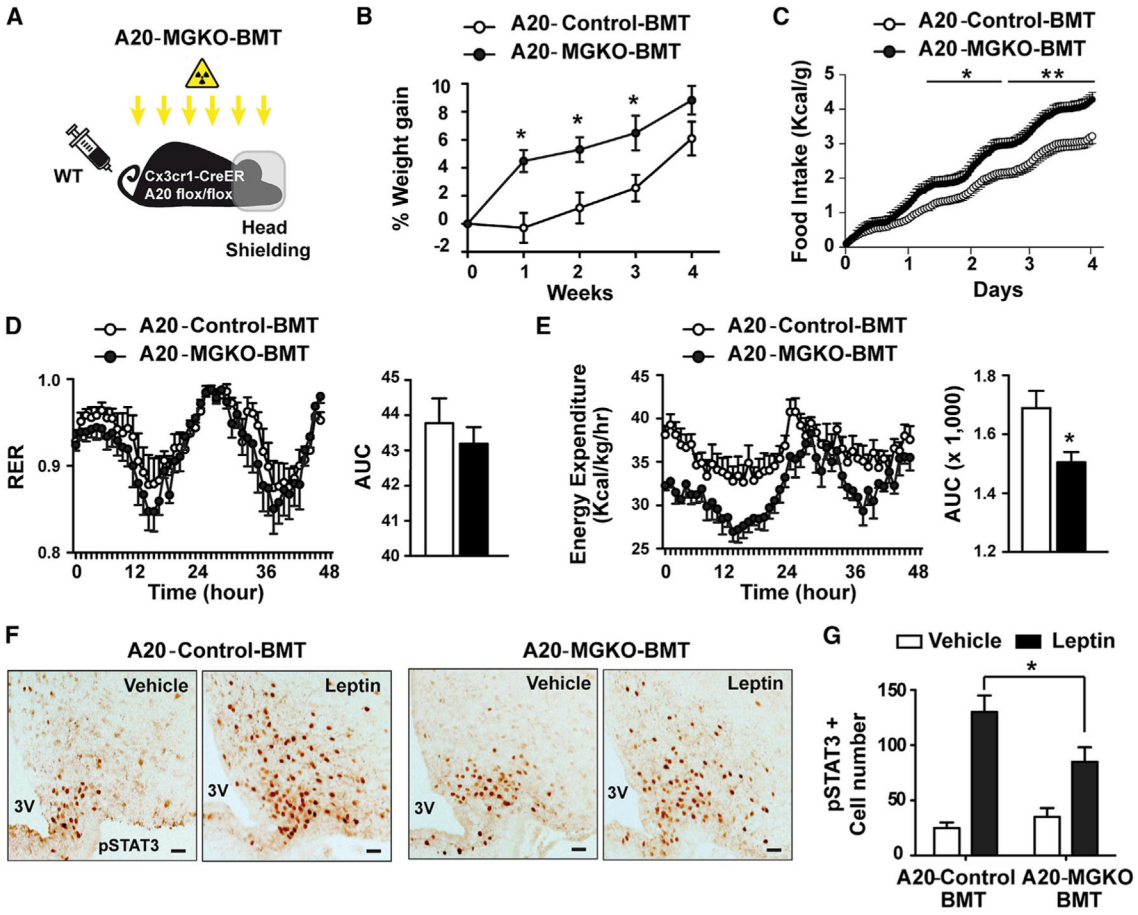

Figure 7. Deleting Microglial A20 Increases Body Weight and Food Intake and Reduces Energy Expenditure

(A) Strategy to restrict A20 deletion to microglia by reconstituting irradiated and head-shielded CX3CR1$^{CreER/+}$: A20$^{F/F}$ mice with WT bone marrow and then treating the resulting mice with tamoxifen following their recovery (A20$^{MGKO-BMT}$).

(B) Spontaneous weight gain following tamoxifen treatment in A20$^{MGKO-BMT}$ mice fed a standard low-fat CD (n = 6, two-way RM-ANOVA, *p < 0.05 versus control).

(C) Increased food intake in CD-fed A20$^{MGKO-BMT}$ mice singly housed in metabolic cages (cumulative intake normalized to intial body weight, n = 6, two-way RM-ANOVA, *p < 0.05, **p < 0.01 versus control).

(D and E) Similar respiratory exchange ratio (RER) values (D) and reduced energy expenditure (E) in A20$^{MGKO-BMT}$ versus control mice (n = 6, *p < 0.05 versus control).

(F) Representative MBH sections showing reduced pSTAT3 staining in the MBH of A20$^{MGKO-BMT}$ mice 45 min after i.p. leptin injection (3 mg/kg). Values are mean ± SEM (scale bar, 20 μm).

(G) Quantification of (F). Values are mean ± SEM. *p < 0.05 versus control. See also Figures S6 and S7.